R34

140 dB Dynamic Range Sub-electron Noise Floor Image Sensor

Sergey Velichko[1], Scott Johnson[1], Dan Pates[1], Chris Silsby[2], Cornelis Hoekstra[2], Ray Mentzer[2], Jeff Beck[2]
[1]ON Semiconductor, Meridian, ID, USA; [2]ON Semiconductor, Corvallis, OR, USA
sergey.velichko@onsemi.com, ph: 408-309-1795

Introduction

In the real world we are surrounded by scenery with dynamic range in excess of 140 dB (10,000,000:1) during daylight and more than 100 dB during night. Sensors for automotive, surveillance, and industrial imaging applications must capture high dynamic range (HDR) images in extreme conditions with temperatures ranging from less than -40°C to more than 105°C. Their performance in both sensitivity and noise should provide for clear images, such that the system may detect a pedestrian or bicyclist on a dark street and stop a vehicle before a possibility of an impact.

Wide adoption of light-emitting diode (LED) based traffic signs and car lights further add to the complex requirements. These signs and lights create artifacts for both rolling shutter and global shutter image sensors, especially during bright daylight and short exposures. For example, some or all information on a sign may not be captured within the image. Advanced automotive image sensors are expected to mitigate this problem.

In this paper we highlight the results of recent work in ON Semiconductor on a new CMOS HDR image sensor capable of handling dynamic ranges in excess of 140 dB, while having improved sensitivity, low thermal noise, and light flicker mitigation, thus suitable for automotive and other emerging applications.

High Dynamic Range

A number of HDR sensor architectures have been reported elsewhere trying to address capturing 120 dB to more than 140 dB dynamic range images, each with their respective pros and cons [1-5]:

- Large capacity photodiode with high readout and thermal noise and generally large pixel size and cost.
- Logarithmic or linear-log photodiode [1] with high readout, fixed pattern, and thermal noise.
- Lateral gate overflow with programmable barriers [2] with high fixed pattern and thermal noise.
- Space separated multiple exposures within frame [3] with corresponding dynamic and color artifacts.
- Split diode space separated variation [4] with corresponding dynamic and color artifacts.
- Our earlier work, sequential within frame three exposures as reflected in [5].

Continuing our earlier research we applied four exposures within the same frame with improved image quality and no artifacts. We considered the multiple exposure approaches as having significant advantages compared to others due to the fact that the same optical pixel is used for all exposures in both low conversion and high conversion gain modes. Also it provided for low readout and thermal noise thus resulting in excellent image quality at all conditions. Dynamic artifacts related to time separated exposures were successfully mitigated with next generation internal image processing. Additionally, we enabled very small sub-row integration time for the shortest exposure, to handle very bright scenery including exposure from the direct sun. Coupled with a wide range programming of exposure ratios and flexibility to use 2, 3, or 4 exposures these improvements allowed to image almost all real life sceneries.

Total signal-to-noise (SNR) four-exposure HDR measurements for the HDR 3µm sensor are shown in Fig. 1 for 60°C junction temperature, tungsten light source, and 16:1 exposure ratio. These measurements clearly showed more than 140 dB dynamic range of the sensor.

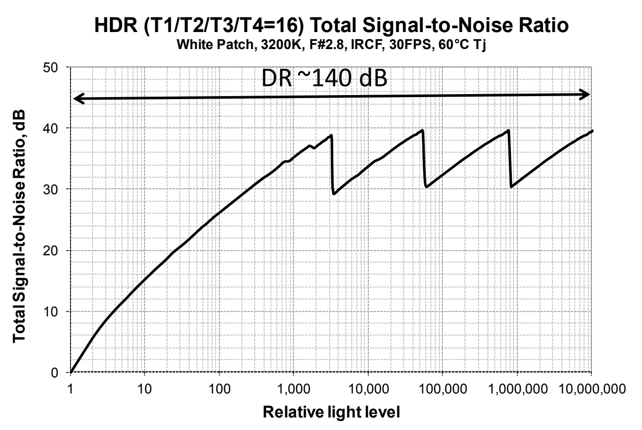

Figure 1. Total SNR at 60C junction temperature

For illustration of the dynamic range within the frame we captured the same scenery in HDR (top) and linear modes (bottom) of operation using the HDR sensor and presented in Fig. 2 below.

The HDR vs. linear image showed more details both in the highlighted part of the image and in the shadows. The difference between HDR and linear image dynamic range was approximately 60 dB.

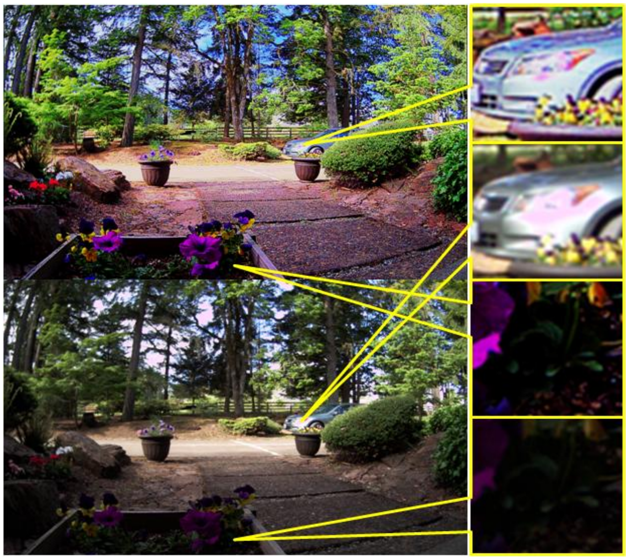

Figure 2. HDR and linear image captures

Pixel Array Performance

High performance requirements for automotive, surveillance and other emerging market applications drive the never-ending push for image sensor improvements. Significant advantage of our HDR sensors is in the usage of Dynamic Response Pixel (DR-Pix) pixel architecture [6] with its ability to significantly boost lowlight performance while maintaining high pixel capacity. The biggest positive change in pixel performance came from switching the manufacturing process from front-side illuminated (FSI) to back-side illuminated (BSI) low thermal noise technology node. That change coupled with optical stack optimization led to a large increase in quantum efficiency (QE) and sensitivity in comparison to previous generation FSI sensors [5-7]. In addition to the sensitivity boost in the visual range we also measured a significant improvement in the near-infrared (NIR) range. Increased NIR sensitivity may be advantageous for some night vision applications.

The low readout noise floor of the sensor was reduced to sub-electron level 0.7e- with correlated multiple sampling (CMS) [8]. In Fig. 3 we presented measurements of readout noise distributions for two- and four-CMS in comparison to baseline non-CMS. It is clearly seen that CMS operations reduced significantly both average level and tail of readout noise.

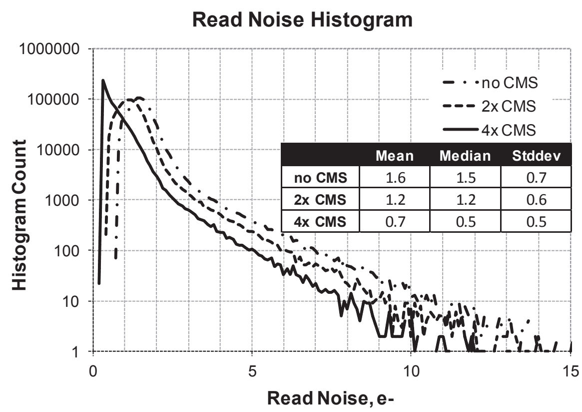

Figure 3. Readout noise distributions with and without CMS

Low thermal noise, increased sensitivity, significant reduction of readout noise, improved fixed pattern noise, and other sources of noise, allowed the new HDR sensor, with smaller pixel size, to outperform the older generation larger pixel size sensor. Luminance SNR serves as a good metric taking into account all noise components and spectral response of sensors. In Fig. 4 we presented luminance SNR plots and equations used for calculations.

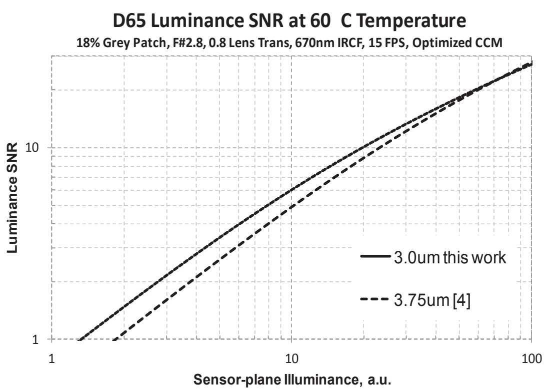

$$\mathrm{LSNR} = \frac{S_{\mathrm{lum}}}{\sigma_{\mathrm{lum}}}$$

$$S_{\mathrm{lum}} = \alpha \cdot R' + \beta \cdot G' + \gamma \cdot B'$$

$$\begin{bmatrix} R' \\ G' \\ B' \end{bmatrix} = \mathrm{CCM} \cdot \begin{bmatrix} R \\ G \\ B \end{bmatrix}$$

$$\sigma^2{}_{\mathrm{lum}} = \alpha^2\sigma^2(R') + \beta^2\sigma^2(G') + \gamma^2\sigma^2(B')$$

$$\alpha = 0.2125,\ \beta = 0.7154,\ \text{and}\ \gamma = 0.0721$$

Figure 4. Luminance SNR comparison

The parameters used in Fig. 6 are: D65 illuminant, 18% grey patch, lens F#2.8, 0.8 lens transmission, 670nm infrared cut filter (IRCF), 15 frames per second (FPS), color optimized ($\Delta E \leq 2.5$) color correction matrix (CCM), measured pixel parameters, and spectral characteristics. They were used to derive the plots at 60°C junction temperature. The smaller 3µm BSI pixel array significantly outperformed 3.75µm FSI pixel array.

In Table 1 we summarized the basic parameters of new HDR sensor in comparison to the older generation sensor [5]. Dynamic range increased up to 140dB. A large boost of QE and sensitivity was measured. The low readout noise floor of new sensors was reduced to 0.7e- with CMS enabled. Very low dark signal non-uniformity (DSNU) was related to low dark current variability. The improvement in DSNU between old and new sensors became more significant with increased temperature.

The pixel array performance of the new generation of HDR sensors allowed for meeting the stringent requirements of different markets and provides for acceptable image quality in wide range of temperatures.

Light Flicker Mitigation

In prior imaging systems [1-7], image artifacts may be caused by flickering lighting and objects with changing illumination in an image frame. For example, such artifacts may include missing parts of an object, edge color artifacts, and object distortion. Examples of objects with changing illumination include light-emitting diode (LED) traffic signs (which can flicker several hundred times per second) and LED stop and head lights of modern cars.

Table 1

Parameter	Unit	[5]	This work
Pixel pitch	µm	3.75	3.0
Sensor technology		FSI	BSI
Dynamic Range [a]	dB	118	Up to 140
Relative Max QE		1.0	1.2
Relative Sensitivity [b]	per pixel	1.0	1.0
Noise Floor [c]	e-	1.8	0.7
Pixel Average Dark Current [d]	pA/cm²	160	59
PRNU	%	0.6	0.6
DSNU [d]	e-	2	0.9
Number of exposures		3	2, 3, 4

[a] 16:1 exposure ratio.
[b] D65 light source, F#2.8 lens, and 670nm IRCF.
[c] At room temperature 25°C.
[d] At 60°C junction temperature.

While electronic rolling shutter (ERS) and global shutter (GS) modes produce images with different artifacts, the root cause for such artifacts is common for both modes of operation. Typically, image sensors acquire light asynchronously relative to the scenery being captured. This means that portions of an image frame may not be exposed for part of the frame duration. This is especially true for bright scenery when integration times are much shorter than the frame time used. Parts of an image frame that are not fully exposed to dynamic scenery may result in object distortion, saturation data loss, and color artifacts. Similar effects may be observed when the camera is moving or shaking during image capture operations.

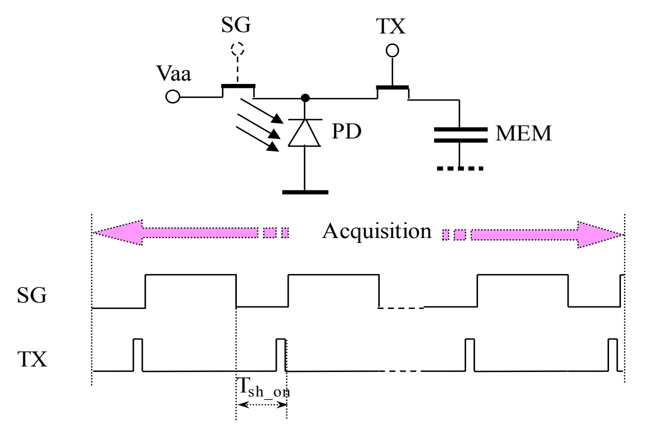

Figure 5. Light flicker mitigation pixel operation

For the sensor, a light flicker mitigation (LFM) method [9] was implemented using a shutter element to realize the electrically programmable pixel sensitivity to avoid these issues in different applications. The generic pixel schematic and timing diagram illustrating the method are shown in Fig. 5. Dynamic shutter reset gate (SG) and transfer gate (TX) operation allowed exposure extended over the frame size thus mitigating any flicker artifacts in an image. This is done by periodic shuttering of photodiode (PD) and charge accumulation in pixel memory (MEM) using SG and TX pulses. Using both number of cycles and duty cycle as variables in row timing signals the effective linear pixel sensitivity can be widely varied. This is particularly unique because no knee points are needed to change the sensitivity, thus simplifying the processing of the image and its interpretation for uses such as traffic sign reading or optical character recognition (OCR). The minimum number of samples and duty cycles were investigated as part of the development.

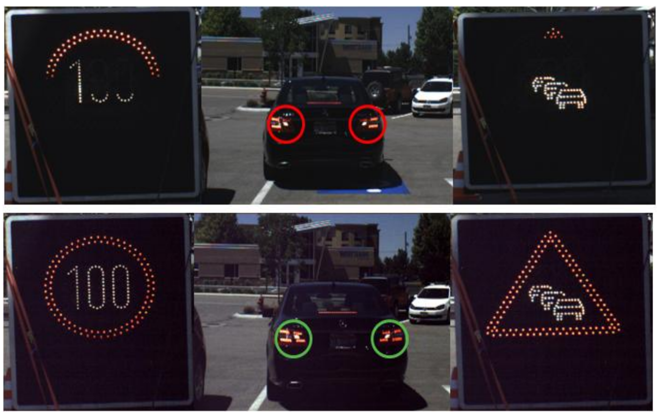

Figure 6. Regular ERS and LFM image captures

Equipped with the LFM technology, the sensor captured all frames without missing information. In Fig. 6 we presented captures of both LED traffic signs and car brake lights in regular ERS (top images) and LFM (bottom images) timing modes.

LFM captured images showed all LEDs being illuminated while ERS captured images showed varying degrees of missing LED information. This missed LED information was especially troublesome when capturing brake or stop lights in critical situations. LFM operation gracefully mitigated these potentially hazardous artifacts. Moreover, LFM technology also successfully demonstrated removing artifacts related to general light flickering including fluorescent lighting.

Conclusion

We have demonstrated the new CMOS HDR sensor with improved performance resulting from increased sensitivity, lower thermal noise, HDR in excess of 140 dB, and light flicker mitigation. The new 3µm pixel array demonstrated performance better than larger 3.75µm pixel array of previous generations at all light levels and temperature conditions. More than 2.5x area scaled improvement in pixel dark current, low 0.7e- readout noise floor, and 2-3x improvement in sensor fixed pattern noise were demonstrated. The addition, LFM capable pixels allowed mitigating effects of flickering lights and LEDs of modern traffic signs and cars. These advancements allow the sensor to satisfy the requirements of different markets including automotive, surveillance, and other emerging areas of application.

Acknowledgement

The authors would like to thank Taner Ozcelik, Ross Jatou, Geoff Ballew, and Chuck McCord for support and proofreading.

REFERENCES

[1] Wei-Fan Chou, Shang-Fu Yeh, Chin-Fong Chiu, and Chih-Cheng Hsieh, "A Linear-Logarithmic CMOS Image Sensor with Pixel-FPN Reduction and Tunable Response Curve", *IEEE Sensors J.*, vol. 14, no. 5, pp. 1625–1632, May 2014.

[2] N. Bock, et al., "A Wide-VGA CMOS Image Sensor with Global Shutter and Extended Dynamic Range", in *Proc. IISW 2005*.

[3] A. Peizerat, et al., "A 120dB DR and 5µm pixel pitch imager based on local integration time adaptation", in *Proc. IISW 2015*.

[4] T. Willassen, et al., "A 1280x1080 4.2µm Split-diode Pixel HDR Sensor in 110nm BSI CMOS Process", in *Proc. IISW 2015*.

[5] J. Solhusvik, et al., "A 1280x960 3.75µm pixel CMOS imager with Triple Exposure HDR", in *Proc. IISW 2009*.

[6] D. Pates, et al., "An APS-C Format 14b Digital CMOS Image Sensor with a Dynamic Response Pixel", in *Proc. ISSCC 2011*.

[7] S. Velichko, "Latest Advancements in CMOS Imaging Sensors", in *Proc. New-Tech 2015*.

[8] N. Kawai and S. Kawahito, "Effectiveness of a correlated multiple sampling differential averager for reducing 1/f noise," *IEICE Electron. Exp*., vol. 2, no. 13, pp. 379–383, July 2005.

[9] C. Silsby, S. Velichko, S. Johnson, Y. P. Lim, R. Mentzer, J. Beck, "A 1.2MP 1/3" CMOS Image Sensor with Light Flicker Mitigation", in *Proc. IISW 2015*.